

## Scars of discrete rotational bands in hot nuclei

R.A. Broglia<sup>1,2,3</sup>, T. Døssing<sup>3</sup>, M. Matsuo<sup>4</sup>, E. Vigezzi<sup>2</sup>, P. Bosetti<sup>1,2</sup>, A. Bracco<sup>1,2</sup>, S. Frattini<sup>1,2</sup>, B. Herskind<sup>3</sup>, S. Leoni<sup>1,2,3</sup>, P. Rasmussen<sup>3</sup>

<sup>1</sup> Dipartimento di Fisica, Università di Milano, Italy

<sup>2</sup> Istituto Nazionale di Fisica Nucleare, Sez. di Milano, Via Celoria 16, I-20133 Milano, Italy

<sup>3</sup> The Niels Bohr Institute, University of Copenhagen, Denmark

<sup>4</sup> Yukawa Institute for Theoretical Physics, Kyoto University, Japan

Received: 24 July 1996

Communicated by W. Weise

**Abstract.** Rotational motion loses its coherence as a function of the nuclear internal excitation energy. The damping process does not proceed in a continuous fashion and scars of discrete rotational bands are found, inbedded in a background of damped rotational states, regardless whether the calculations are carried out using effective or “random” forces. The complexity of the damping mechanism is revealed in the lineshape of the ridges in the  $\gamma$ - $\gamma$  correlation spectrum.

**PACS:** 21.60.Cs; 21.60.Ev; 23.20.Lv

Collective rotation is a well known behaviour of cold nuclei (cf. e.g. [1]), but is less understood when the nucleus becomes internally excited. Discrete transitions are no longer observable and information about rotational motion must be extracted from a spectrum of  $\gamma$ -rays that appears continuous. The observation that only a fraction of the rotational transitions arise from the decay of the compound nucleus along discrete rotational bands, testifies to the fact that rotational motion becomes damped in hot nuclei (cf. e.g. [2–6]). Rotational damping has its atomic analog in the temperature-dependent line broadening observed in Nuclear Magnetic Resonance (NMR) [7].

The cranked mean field [8] provides a microscopic basis for describing the structure of rotating nuclei. Excited bands correspond to quasiparticle excitations. As the number of quasiparticles increases, rotational bands become close in energy, and the residual interaction acting among them gives rise to compound states which are superposition of many bands. Still, rotational phase correlations may be kept over neighbouring values of the angular momentum differing by two units. Often, however, the different many-quasiparticle configurations of the compound nucleus eigenstates respond differently to changes in the rotational frequency, that is they display different alignment, leading to changes of the Hamiltonian with  $\Delta I = 2$  which are strong enough to weaken the phase correlations and generate a fragmentation of the rotational decay out of each state. This leads to the damping of the rotational motion. Theoretical studies of rotational damping have focused on the conditions of compound nucleus

formation and the associated level statistics at one angular momentum, as well as on the rotational strength function of one decay-step, and its fluctuations [7,9–15]. However, the most detailed information is contained in double- and higher-fold  $\gamma$ -coincidences spectra (cf. e.g. [16]).

In what follows we present results of cranked shell model calculations where the rotational bands interact via two-body forces [17]. It shall be concluded that the phase coherence existing between the members of rotational bands is not lost in a uniform fashion with increasing intrinsic excitation energy, but displays large variations from state to state. Scars of this coherence may be found in regions where the average distance between unperturbed rotational bands is many times smaller than the average rotational damping width. This result may be used at profit, also in other finite quantal systems, in particular molecular clusters (cf. e.g. [20]) and eventually Bose-Einstein condensates [21], to learn about the role individual quantal configurations have on the rotation of the system as a whole.

In keeping with the cranking model, each rotational band  $\mu$  corresponds to a intrinsic np-nh configuration. We construct such configurations based on the diabatic single particle basis obtained from the cranked Nilsson Hamiltonian  $h_{crank} = h_{Nilsson} - \omega j_x$ . We do not include the pairing potential since we restrict our analysis to the high spin region ( $I > 30$ ) where the pairing gap is expected to be small or even vanish, particularly for the many-particle many-hole configurations we are mostly concerned with. The energy of the bands in the laboratory frame is given by  $E_\mu(I) = E'_\mu(\omega) + \omega J_{x,\mu}(\omega)$  with the total routhian  $E'_\mu(\omega)$  and a constraint  $J_{x,\mu}(\omega) = I$  on the rotational frequency  $\omega$  on the rotational, where  $J_{x,\mu}(\omega)$  is the expectation value of the angular momentum  $J_x$  along the rotation axis. Using the diabatic basis, which displays a smooth dependence on rotational frequency, it is possible to approximate the energy [15] by

$$E_\mu(I) = E'_\mu(\omega_I) + \omega_I I + \frac{(I - J_{x,\mu}(\omega_I))^2}{2J_\mu^{(2)}}, \quad (1)$$

where the average rotational frequency  $\omega_I$  obeys the angular momentum condition  $\langle J_x \rangle_{av} = I$ ,  $J_\mu^{(2)}$  being the dynamic moment of inertia. We then obtain compound states

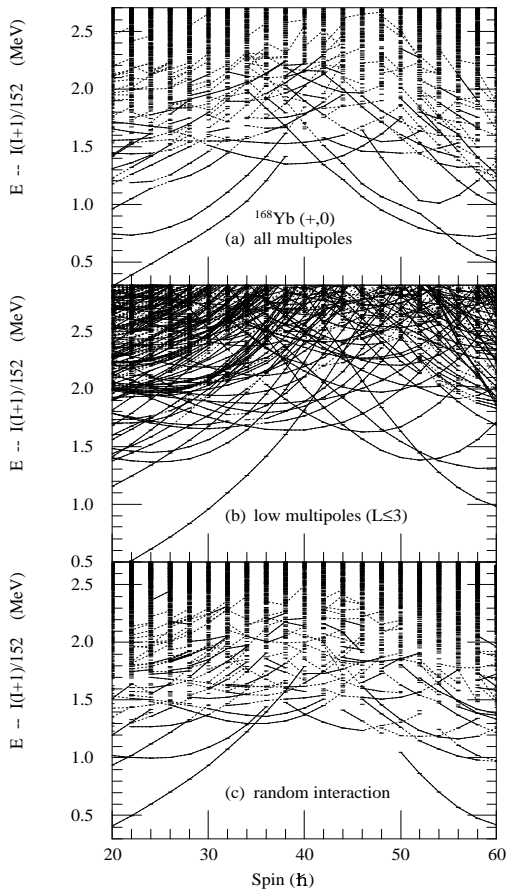


**Fig. 1a-c.** The compound energy levels  $|\alpha(I)\rangle$  of  $^{168}\text{Yb}$  are shown as a function of angular momentum, subtracting the rotational energy of a rigid rotor of moment of inertia  $\mathcal{I} = 76 \hbar^2 \text{MeV}^{-1}$ . **a** refers to the calculation carried out diagonalizing the full surface delta interaction, while in **b** only the multipoles  $\lambda \leq 3$  are considered. **c** refers to the results of a calculation performed with a random force whose average mean square root of the matrix elements was set equal to  $12 \text{keV} \approx \sqrt{V_{\mu\mu'}^2} >_{\lambda>3}^{1/2}$

$|\alpha(I)\rangle = \sum_{\mu} X_{\alpha\mu}(I) |\mu(I)\rangle$ , by diagonalizing the shell model hamiltonian with a surface-delta interaction of standard strength [22]. We have used a basis containing  $10^3$  intrinsic states. The truncation used in the size of the basis states has been checked to give stable results for the lowest 300 levels of each parity and signature, which cover an interval in intrinsic excitation energy, that is of excitation energy above the yrast line, of approximately 2.2 MeV.

The stretched E2 transition probability  $P_{\alpha\alpha'}$  connecting two compound states  $|\alpha(I)\rangle$  and  $|\alpha(I-2)\rangle$  was calculated as

$$P_{\alpha\alpha'} = \left| \sum_{\mu} X_{\alpha\mu}(I) X_{\alpha'\mu}(I-2) \right|^2, \quad (2)$$

where we have assumed that the transition follows the unperturbed bands so that the E2 operator is diagonal with respect to  $\mu$ . The calculations were carried out for the case of the nucleus  $^{168}\text{Yb}$  for which many experimental efforts have been carried out in the study of rotational damping, efforts which seem to lead to the conclusion that the line shape of rotational decay is composed of a number of strength functions of different widths [23,24].

The results of the calculation for the levels with parity + and signature 0 are displayed in Fig 1(a) as a function of the angular momentum in the interval  $20 < I < 60$ . If the quadrupole decay out of a compound nuclear state at spin  $I$  populates with a probability larger than 70% a single state at spin  $I-2$ , the two states are joined by a continuous line. If this probability is in the range between 70% and 50%, the levels are joined by a dashed line. The region of lowest excitation energy at each spin is dominated by rotational bands with strong E2-transitions. For each set of three consecutive angular momenta,  $(I+2, I, I-2)$ , about 3 to 9 such “strong” rotational bands connecting states at the three spins are predicted by the calculations. They correspond to the rotational bands found in the study of discrete gamma spectroscopy. With increasing excitation energy, the quadrupole transitions fan out, reflecting the loss of correlation between different  $I$ -spin states. The damping process shows however conspicuous irregularities. In fact, even at intrinsic excitation energies as high as 1.5 MeV, where the distance between unperturbed rotational levels is of the order of keV’s, while typical matrix elements between bands have a value of the order of 20 keV, we find continuous or dashed lines joining two, in some case three states at spin  $I+2$ ,  $I$  and  $I-2$ , scars of discrete bands in a region of the spectrum controlled by rotational damping. In connection with the discussion below, and in keeping with the results of ref. [14], we have repeated the calculations making use of only the low ( $\lambda \leq 3$ ) multipoles of the surface-delta interaction. The results obtained are displayed in Fig. 1b. No rotational damping is observed in this case. This is because the low-multipole components of the surface-delta interaction lead only to mean field effects and consequently do not mix rotational bands democratically. Mixing states  $|\mu\rangle$  which behave similarly as a function of rotational frequency leads to a decay pattern of the corresponding  $|\alpha\rangle$ -states which still displays discrete, sharp transitions, essentially identical to those observed in the collective, quadrupole rotational decay associated with the  $|\mu\rangle$ -states.

The presence of scars of discrete bands observed in Fig. 1a in a region of the  $E-I$  plane controlled by rotational damping is quite interesting and may refer to general properties of the motion of finite quantal systems, being these atomic nuclei, metal clusters, fullerenes, Bose-Einstein condensates, etc. Among these properties one can mention that the density of the levels which couple directly to a given  $|\mu\rangle$ -state through the two-body residual interaction is, already at an intrinsic excitation energy of 1.2 MeV, considerably smaller ( $\approx 10 \text{MeV}^{-1}$ ) than the total density of levels ( $\approx 10^2 \text{MeV}^{-1}$ ). Second, because of the finite size of the nucleus, and depending on its shape, the sequence of single-particle levels appears to be locally irregular both in energy and in quantum numbers due to the deformation and to the rotational degrees of freedom. Intruder states, that is, states whose properties are different from those of the states nearby, ensue. This feature will also be present in the multi-particle, multi-hole excitations of the system, and can explain the local incapacity of certain states  $|\mu\rangle$  to mix with states nearby (background) other than those having essentially the same properties as the state  $|\mu\rangle$  has. In other words, a typical  $|\mu\rangle$ -state may, at some value of excitation energy and spin, be surrounded by equally typical  $|\mu\rangle$ -states displaying

rather different properties, like for example alignment. It is sufficient that this happens within an energy range of the order of the average value of the matrix elements of the residual interaction ( $\langle V_{\mu\mu'}^2 \rangle^{1/2} \approx 19$  keV), that the state  $|\mu\rangle$  in question will not mix with other states, or, in any case, mix only with other intruder states all displaying similar physical properties. While the details of which matrix elements of the two-body residual interaction are zero or, in any case, small depend on the detailed structure of the nucleus under discussion, the presence of isolated rotational bands which do not mix, or mix over a few spins only within a selected group of bands, does not. This scenario seems to be confirmed by the results shown in Fig. 1c where the results obtained with a random force, whose average mean square root value was set approximately equal to  $\langle V_{\mu\mu'}^2 \rangle^{1/2}$ , that is the part of the residual two-body interaction which does not lead to any significant mean field effect and mixes democratically all rotational bands. The overall rotational pattern observed in Fig. 1c is very similar to that seen in Fig. 1a.

The  $\gamma$ - $\gamma$  correlation spectrum testifies to the variety of phenomena associated with the onset of rotational damping. The peaks forming the ridge along the diagonal display a line shape which is the result of a subtle combination of the phenomena described above. This can be seen from Fig. 2, where the spectra resulting from cuts taken perpendicular to the diagonal of the two-dimensional  $\gamma$ - $\gamma$  correlation plot are displayed for energy bins centered around different values of the excitation energy above yrast. In all cases the transition  $\gamma_1$  connects spin  $I+2$  with spin  $I$  while  $\gamma_2$  corresponds to the E2-decay between spin  $I$  and spin  $I-2$ . In order to have good statistics, we have summed up the spectra obtained at spins comprised between  $I=50$  and  $I=30$ . The bins contain: a) the lowest 20 levels, b) levels 21–40, c) levels 41–60, d) levels 61–80 and e) levels 251–300, corresponding to the intrinsic energy intervals  $U=0-1.2$  MeV, 1.2–1.45 MeV, 1.45–1.6 MeV, 1.6–1.7 MeV and 2.2–2.25 MeV respectively. A line shape made out of the sum of a number of functions displaying different widths is apparent. This can be seen more clearly by displaying the line-shapes associated with two-fold coincidence transitions such that the product probability  $P_1P_2$  of the first ( $P_1$ ) and second ( $P_2$ ) transition probabilities are contained between different boundaries. This is shown in Fig. 2b for the bin corresponding to  $1.2$  MeV  $< U < 1.45$  MeV. The narrow component of the strength function ( $P_1P_2 > 0.3$ ) arises from the scars of rotational bands present at rather high excitation energy above yrast (short traits connecting 3–4 states in Fig. 1a). The width of this component is of the order of 20–30 keV and can be correlated with the distribution of values of the moments of inertia associated with well-defined discrete, near-yrast states (continuous lines in Fig. 1a). The next broader component ( $0.03 < P_1P_2 < 0.3$ ), displaying a width between 50 and 80 keV, arises from transitions whose intensity is lower than that of the scars shown in Fig. 1a, but is still higher than the average intensity ( $P_1P_2 \sim 0.01$ ) expected for damped transitions. The width of this component changes with the energy interval covered by the bin, and essentially reflects the compound nucleus damping width  $\Gamma_\mu$ . Finally, a broad structure is observed ( $P_1P_2 < 0.03$ ) with a width of the order of 200–250 keV. This width arises from the decay of

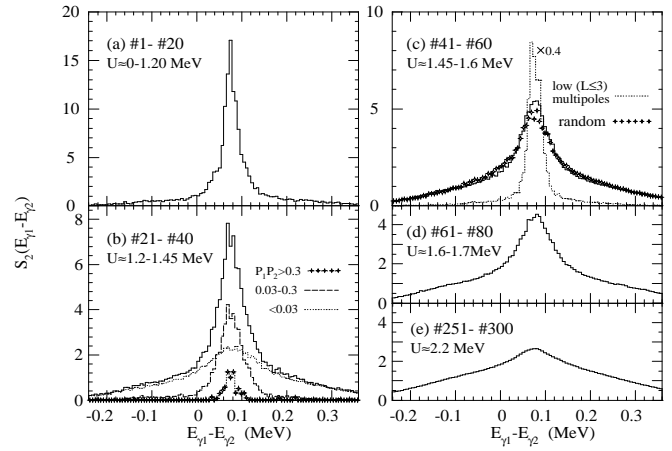


**Fig. 2a–e.** Spectra obtained from the energy difference of two consecutive transitions  $I+2 \rightarrow I \rightarrow I-2$  between the calculated energy levels. The spectra include the transitions with  $30 < I < 50$  in order to obtain good statistics. The continuous curves in **a–e** are constructed from the transitions originating from the lowest 20 levels above yrast **a**, from the levels 21–40 **b**, from the levels 41–60 **c**, from the levels (61–80) **d** and from the levels 251–300 **e**

states which from spin  $I$  populate a large number of states at spin  $I-2$ , and can be associated with the “real” rotational damping width  $\Gamma_{rot}$ . Its value is close to the value of the rotational damping width calculated [12] neglecting the correlations existing between consecutive transitions. As the energy is progressively increased the strength function associated with “real” rotational damping is the only component that survives in the two-fold correlated rotational decay pattern, as can be seen in Fig. 2e. In keeping with the rotational pattern decay shown in Fig. 1c, similar results for the  $\gamma$ - $\gamma$  strength function as those obtained from the diagonalization of the surface-delta interaction were obtained making use of the random interaction (cf. Fig. 2c), while the low ( $\lambda \leq 3$ ) multipoles (cf. Fig. 1b) lead to a narrow distribution typical of well-defined rotational bands. In experimental energy correlation spectra, the narrow component of the ridge, stemming from transitions along low lying bands and scars, is clearly present in both the 2 dimensional and 3 dimensional versions [23,24]. Especially, the strong fluctuations of the spectra on the ridges are well accounted for quantitatively by the present model [25].

We conclude that the onset of rotational damping is not a sharp event taking place at a given excitation energy above the yrast band, but proceeds in steps over a broad intrinsic excitation energy region extending from about 1 MeV to 1.5–2 MeV. The predictions of the model can be tested experimentally studying the line-shape of the first ridge in the  $\gamma$ - $\gamma$  correlation spectrum observed in the decay of hot nuclei, making use of the new generation of  $4\pi$ -detector arrays like Gammasphere or Euroball.

## References

1. Bohr, A., Mottelson, B.R.: Nuclear Structure Vol. II, Benjamin, Reading, Mass. (1975)
2. Banashik, M.V., et al.: Phys. Rev. Lett. **34**, 892 (1995)
3. Deleplanque, M.A., et al.: Phys. Rev. Lett. **41**, 1105 (1978)

4. Hübel, H., et al.: Phys. Rev. Lett. **41**, 791 (1978)
5. Diamond, R.M., Stephens, F.S.: Annu. Rev. Nucl. Part. Sci. **30**, 85 (1985)
6. Herskind, B., in: Proc. Int. School of Physics, Varenna, Enrico Fermi Course LXXXVII, Amsterdam: North Holland 1984
7. Broglia, R.A., et al.: Phys. Rev. Lett. **58**, 326 (1987)
8. Bengtsson, R., Frauendorf, S.: Nucl. Phys. **A314**, 27 (1979); **A327**, 137 (1979)
9. Leander, G.A.: Phys. Rev. **C25**, 2780 (1982)
10. Bacelar, J.C., et al.: Phys. Rev. Lett. **55**, 1985 (1985)
11. Draper, J.E., et al.: Phys. Rev. Lett. **56**, 309 (1986)
12. Lauritzen, B., et al.: Nucl. Phys. **A457**, 61 (1986)
13. Egido, J.L., Faessler, A.: Z. Phys. **A339**, 339 (1991); Egido, J.L., Weidenmüller, H.A.: Phys. Lett. **208**, 58 (1988), Phys. Rev. **C39**, 2398 (1989); Egido, J.L.: Phys. Lett. **B232**, 1 (1989)
14. Matsuo, M., et al.: Phys. Rev. Lett. **70**, 2694 (1993)
15. Åberg, S.: Phys. Rev. Lett. **64**, 3119 (1990)
16. Herskind, B., et al.: Phys. Rev. Lett. **68**, 3008 (1992); Åberg, S.: Prog. Part. Nucl. Phys. Vol. 28, p. 11, Pergamon 1992
17. In keeping with the fact that rotational damping is controlled by the mixing of rotational bands displaying different alignments while compound damping is the result of a democratic mixing of rotational states, it can be concluded that rotational damping and compound damping have completely different origin and are, as a matter of principle, not related to each other (cf. e.g. [18,19]). When the width  $\Gamma_{\mu}$  of compound states is larger than the average separation energy between intrinsic configurations, and the spread in rotational frequencies ( $2 \Delta\omega$ ) due to the spread in the alignments is larger than  $\Gamma_{\mu}$  the rotational damping width turns out to be independent of the strength of the residual interaction and equal to  $2 (2\Delta\omega)$  [12]
18. Mottelson, B.R.: Nucl. Phys. **A557**, 717c (1993)
19. Døssing, T., et al.: Phys. Rep. **268C**, 1 (1996)
20. Bertsch, G.F., Broglia, R.A.: Oscillations in Finite Quantum Systems. Cambridge: Cambridge University Press 1994
21. Stringari, S.: Phys. Rev. Lett. **76**, 1405 (1996)
22. Faessler, A.: Fortschr. Physik **16**, 309 (1968)
23. Herskind, B., et al.: Phys. Lett **B276**, 4 (1992)
24. Leoni, S., et al.: Nucl. Phys. **A 587**, 513 (1995)
25. Bracco, A., et al.: Phys. Rev. Lett. **76**, 4484 (1996)